

Evidence of Graphitic AB Stacking Order of Graphite Oxides

Hae-Kyung Jeong,^{*,†} Yun Pyo Lee,[†] Rob J. W. E. Lahaye,[†] Min-Ho Park,[‡]
 Kay Hyeok An,[§] Ick Jun Kim,^{||} Cheol-Woong Yang,[‡] Chong Yun Park,[†]
 Rodney S. Ruoff,[⊥] and Young Hee Lee^{*,†}

BK21 Physics Division, Institute of Basic Science, Center for Nanotubes and Nanostructured Composites, Sungkyunkwan University, Suwon 440-746, Korea, School of Advance Materials and Engineering, Sungkyunkwan University, Suwon 440-746, Korea, Material & Development Department, Jeonju Machinery Research Center, Jeonju 561-844, Battery Research Group, Korea Electrotechnology Research Institute (KERI), Changwon 641-120, Korea, and Department of Mechanical Engineering, College of Engineering, University of Texas, 1 University Station C2200, Austin, Texas 78712

Received August 28, 2007; E-mail: outron@skku.edu; leeyoung@skku.edu

Abstract: Graphite oxide (GO) samples were prepared by a simplified Brodie method. Hydroxyl, epoxide, carboxyl, and some alkyl functional groups are present in the GO, as identified by solid-state ¹³C NMR, Fourier-transform infrared spectroscopy, and X-ray photoemission spectroscopy. Starting with pyrolytic graphite (interlayer separation 3.36 Å), the average interlayer distance after 1 h of reaction, as determined by X-ray diffraction, increased to 5.62 Å and then increased with further oxidation to 7.37 Å after 24 h. A smaller signal in ¹³C CP-MAS NMR compared to that in ¹³C NMR suggests that carboxyl and alkyl groups are at the edges of the flakes of graphite oxide. Other aspects of the chemical bonding were assessed from the NMR and XPS data and are discussed. AB stacking of the layers in the GO was inferred from an electron diffraction study. The elemental composition of GO prepared using this simplified Brodie method is further discussed.

I. Introduction

Graphene sheets have extraordinary electronic transport properties, and with reference to the in-plane properties of graphite, they should also have remarkable thermal conductivity and mechanical stiffness in tension.^{1,2} Recently, stable aqueous dispersions of polymer-coated graphene-based sheets have been prepared via exfoliation of graphite oxide (GO) in water, coating with poly(sodium-4-pyrene sulfonate), and in situ reduction of the coated graphene oxide sheets.³ This is a chemical route to forming layers similar in type to graphene and is one example of why it is important to understand the chemical structure and also chemistry of both GO and exfoliated GO (thus, graphene oxide) sheets.

The first synthesis and thus discovery of GO was described by Brodie in 1859.⁴ There are now three synthesis methods typically in use: that of Brodie,⁵ Staudenmaier,⁶ and Hummers

and Offeman.⁷ In all three, the layers in graphite are extensively oxidized by oxidative treatment in fuming acids. The interlayer distance increases from 3.35 Å of the starting graphite to 7–10 Å, depending on the extent of oxidation and the interlamellar water content. Boehm and Scholz say that the Staudenmaier method is the slowest and gives the lightest colored GO, whereas the Hummers and Offeman method is the fastest and gives a brownish GO.⁸ Both methods have been known⁸ to produce unstable GOs with a high degree of contamination and degradation. GO synthesized with Brodie's method is bright in color and is very stable with a low contamination. In addition, it has the smallest interlayer distance among the various methods.⁸

The possible presence of a variety of functional groups for the basal plane of the layers of graphite oxide produced by these methods has been discussed: epoxide, carbonyl, quinone, ketone, and hydroxyl groups.^{9–17} These functional groups may induce corrugation or local "puckering" of the carbon skeleton.^{10,11,14} There is hardly universal agreement about the type and spatial distribution of functional groups.¹⁴ Furthermore, the "flatness" of the layers in various graphite oxides is still under

[†] Physics Division, Sungkyunkwan University.

[‡] School of Advance Materials and Engineering, Sungkyunkwan University.

[§] Jeonju Machinery Research Center.

^{||} KERI.

[⊥] University of Texas at Austin.

- (1) Novoselov, K. S.; Geim, A. K.; Morozov, S. V.; Jiang, D.; Zhang, Y.; Dubonos, S. V.; Grigorieva, I. V.; Firsov, A. A. *Science* **2004**, *306*, 666–669.
- (2) Zhang, Y.; Tan, Y.-W.; Stormer, H. L.; Kim, P. *Nature* **2005**, *438*, 201–204.
- (3) Stankovich, S.; Piner, R. D.; Chen, X.; Wu, N.; Nguyen, S. T.; Ruoff, R. S. *J. Mater. Chem.* **2006**, *16*, 155–158.
- (4) Brodie, B. C. *Philos. Trans. R. Soc. London* **1859**, *149*, 249–259.
- (5) Brodie, B. C. *Ann. Chim. Phys.* **1860**, *59*, 466–471.

- (6) Staudenmaier, L. *Ber. Dtsch. Chem. Ges.* **1898**, *31*, 1481–1487.
- (7) Hummers, W. S.; Offeman, R. E. *J. Am. Chem. Soc.* **1958**, *80*, 1339.
- (8) Boehm, H. P.; Scholz, W. *Justus Liebigs Ann. Chem.* **1965**, *691*, 1–4.
- (9) Hofmann, U.; Holst, R. *Ber. Dtsch. Chem. Ges.* **1939**, *72*, 754–771.
- (10) Ruess, G. *Monatsch. Chem.* **1946**, *76*, 381–417.
- (11) Scholz, W.; Boehm, H. P. *Z. Anorg. Allg. Chem.* **1969**, *369*, 327–340.
- (12) Mermoux, M.; Chabre, Y.; Rousseau, A. *Carbon* **1991**, *29*, 469–474.
- (13) Left, A.; He, H.; Forster, M.; Klinowski, J. *J. Phys. Chem. B* **1998**, *102*, 4477–4482.
- (14) Szabó, T.; Berkesi, O.; Forgó, P.; Josepovits, K.; Sanakis, Y.; Petridis, D.; Dékány, I. *Chem. Mater.* **2006**, *18*, 2740–2749.

discussion in the literature.^{11–14} Another question is the nature of the stacking order of the layers in various graphite oxides. Unlike graphite that can have, for example, AB stacking order, the stacking of the layers in GO is typically assumed to have no long-range order. However, a sixfold symmetry of stacking in graphite oxides synthesized by all three methods has been observed, which led to the conclusion that the layers in such GO samples had a turbostratic random ordering.^{11,18}

The purpose of this article is to develop further understanding of the structural properties of graphite oxides, in particular of the type generated by our simplified Brodie method. We have done a systematic study by combining X-ray diffraction (XRD), nuclear magnetic resonance (NMR); solid-state and proton cross-polarization/magic-angle sample spinning, thus SS ¹³C NMR and ¹H CPMAS NMR), elemental analysis (EA), X-ray photoemission spectroscopy (XPS), Fourier-transform infrared spectroscopy (FTIR), Raman spectroscopy, and selected area electron diffraction (SAED) in a transmission electron microscope (TEM). The epoxide, hydroxyl, carboxyl, and alkyl functional groups were thereby identified, and it was possible also to learn about their spatial distribution on the carbon skeleton. The epoxide and hydroxyl groups are near each other, and the carboxyl and alkyl groups are more likely to be located at the edges in graphite oxide as made here. The SAED patterns that were acquired exhibit a sixfold symmetry with a perfect hexagonal structure, indicating that the layers are nearly flat and preserve AB stacking order, similar to that of graphite.

II. Sample Preparation and Experimental Methods

Graphite oxide samples were synthesized from graphite (99.999% stated purity, –200 mesh, Alfar Aesar) following Brodie's method,⁵ except that neither an ice bath nor a dropping funnel was used. Graphite (1 g), fuming nitric acid (20 mL), and sodium chloride oxide (8.5 g) were mixed at room temperature without the subsequent aging typically used in the conventional "Brodie's method". The mixture was stirred for 24 h. Washing, filtration, and cleaning were done in the same way as described by Brodie.⁵ We refer to the sample obtained after 24 h of oxidation as GO1, and after 48 h of oxidation as GO2. A part of GO1 was heat-treated at 200 °C for 1 h in 100 sccm of Ar environment; the initial pressure was 1 mTorr before introduction of the sample, and the pressure with Ar(g) during exposure of the sample was 550 mTorr. The heating rate was 50 °C/min starting from room temperature, and the sample (GO1_200C) was cooled with the same rate. The three samples (GO1, GO2, and GO1_200C), along with the precursor graphite (PG) as a reference, were studied, and the results of their characterization are described herein.

Powder X-ray diffraction (D8 FOCUS 2.2 KW, Bruker AXS) with a Cu anode (1.54 Å) was used to fit the average interlayer distance in these GOs, and their physical structure was assessed from scanning electron microscope (SEM, JEOL JSM6700F) images acquired at 5–15 keV. Elemental analyses were obtained (C, O, H, N, S; EA1110, CE Instrument). Raman spectra (Renishaw, RM1000-InVia; excitation energy of 2.41 eV (514 nm)) were obtained to study possible defect formation. The FTIR (Bruker IFS-66/S), XPS (ESCA2000, VG Microtech), and 600 MHz SS ¹³C NMR (UnityINOVA600, Varian) instruments were all operated at room temperature. Each sample for FTIR was mixed with KBr and then finely ground to make a pellet. To distinguish if there was a moisture effect by their exposure in ambient, the pellets were next dried in an oven at 80 °C for a week and FTIR was immediately taken again. TEM (FEJEM 2100F, JEOL, 200 keV) images were acquired from samples deposited onto a holey carbon support film. Samples were sonicated in ethanol for 10 min in a bath-type sonicator (Power Sonic 505, Hwashin), and the resulting GO suspension was then dropped onto a 200 mesh Cu grid (JEOL)

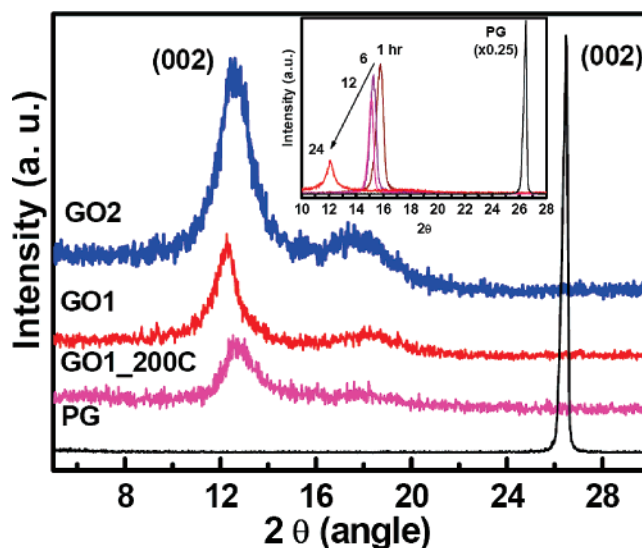


Figure 1. XRD patterns of GOs and the PG used to make them. Inset shows XRD as a function of oxidation time at 1, 6, 12, and 24 h. In both cases, the intensity of the PG peaks was multiplied by 0.25.

having a holey carbon support film. SAED was done in the TEM, and the electron beam size was about 500 nm.

III. Results and Discussion

Figure 1 shows the XRD patterns of the GO samples and the precursor graphite. The XRD patterns of the GO samples are all offset by 3000 counts/s, and the intensity of the graphite pattern was multiplied by 0.25. The (002) peak for each GO sample yields an interlayer separation of about 7 Å. The influence on *d*-spacing of the time of exposure to the fuming nitric acid on the (originally) precursor graphite changes dramatically with time, as shown in the inset of Figure 1. After 1 h of exposure, the (002) peak position of graphite has moved significantly, to a *d*-spacing value of 5.62 Å that then gradually increases to 5.80, 5.85, and 7.37 Å as the exposure time was increased to 6, 12, and then 24 h. A radical expansion of the interlayer distance thus takes place at an early stage during the oxidation process. The rate of increase in interlayer spacing is much smaller between 1 and 6 h vs between 0 and 1 h and evidently reaches a plateau value of 7.2 Å after 24 h; thus, the maximum rate of increase must lie between 0 and 1 h. Continuing the oxidation for a total time of 48 h (GO2) did not change the interlayer distance as compared to that at 24 h, which is consistent with previous work.¹⁴ The full width at half-maximum (FWHM) of the (002) XRD peak is significantly larger for GO1 (± 0.35 Å) than that for the graphite (± 0.015 Å). A shoulder was observed around 18°, indicating that some portion of the graphite oxide layer was not fully intercalated, although the interlayer distance of about 7 Å is clearly dominant. The average in-plane lattice constant for the three GO samples was 1.43 ± 0.015 Å from fitting the (100) XRD peak (Supporting Information S1), similar to 1.426 ± 0.005 Å in graphite.

An SEM image of graphite clearly shows "chunky" layered structures (Figure 2a). With a treatment time of 24 h, these layered structures were exfoliated and transformed into smaller-sized flakes (Figure 2b). With a treatment time of 48 h (GO2), the structures were further exfoliated as shown in Figure 2c. With exposure of GO1 at 200 °C under Ar(g) for 1 h, ordered

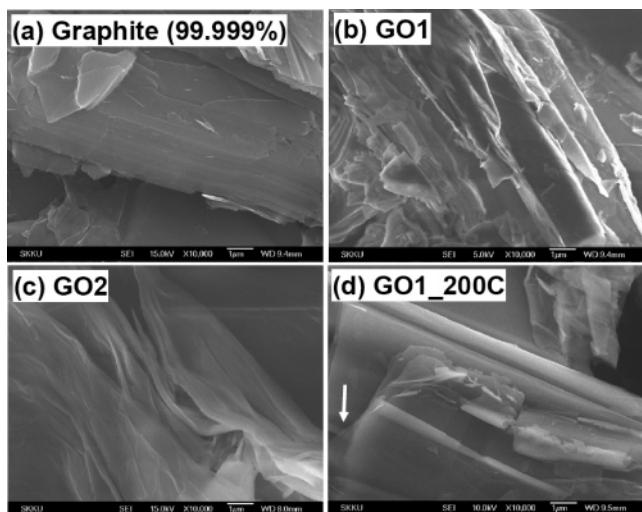


Figure 2. SEM images of GOs and PG. Accelerating electron energies for GO2 and PG are 15.0 and 5.0 kV for GO1, and 10.0 kV for GO1_200C. All images show a scale bar of 1 μm .

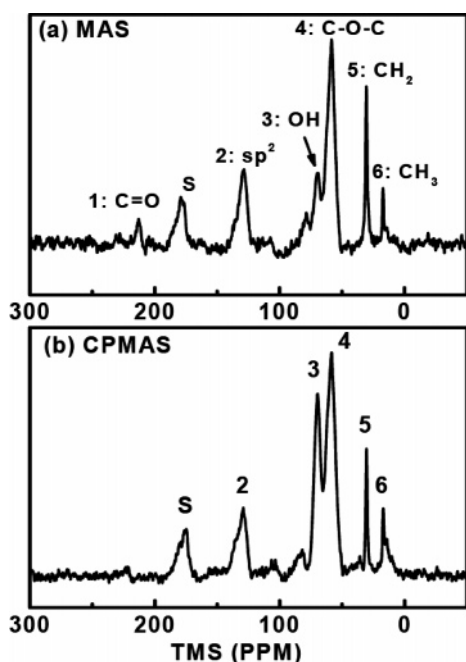


Figure 3. ^{13}C NMR spectra of GO1 with (a) MAS condition and (b) proton decoupling and MAS mode (CPMAS). The peaks 1, 2, 3, 4, 5, and 6 correspond to carbon bonded to carbonyl, sp^2 -hybridized carbon, hydroxyl, epoxide, CH_2 , and CH_3 , respectively.

layered structures similar to those seen in the graphite sample resulted but the exfoliated layered structures still remained unchanged as indicated by the arrow (Figure 2d).

To identify the functional groups that were present from the fuming nitric acid treatment employed here, high-resolution solid ^{13}C NMR measurements were performed with magic-angle spinning (MAS) and ^1H CPMAS. Figure 3 shows MAS ^{13}C NMR spectra: five main peaks were observed. The peaks at 128.5 (peak 2), 69.1 (peak 3), and 58.4 ppm (peak 4) are assigned as sp^2 -hybridized carbon, hydroxyl, and epoxide groups, respectively, thus agreeing with the previous reports.^{12–15} Three additional peaks were assigned to carbonyl at 212.9 ppm

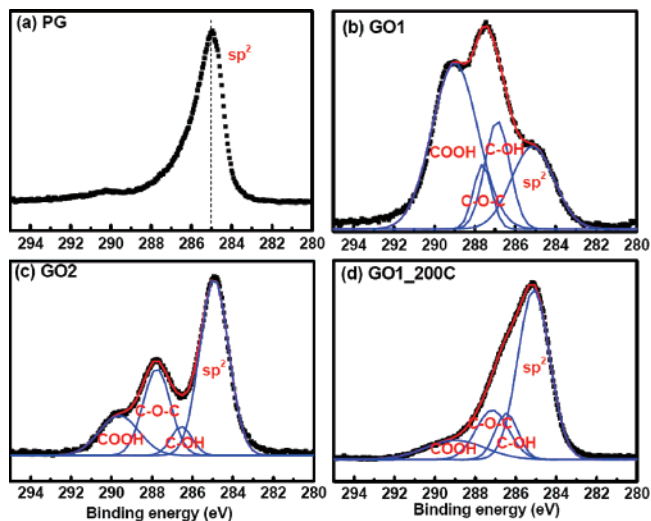


Figure 4. XPS spectra of C1s. The spectra are deconvoluted into four peaks of sp^2 , COOH, C–OH, and C–O–C groups.

(peak 1), CH_2 at 30.5 ppm (peak 5), and CH_3 at 17.2 ppm (peak 6). These peaks have not been observed in GO samples prepared by the standard Staudenmaier,^{12,15} Brodie,^{12,14} or Hummers methods.^{12,13} The epoxide, hydroxyl, and sp^2 -hybridized carbon peaks appeared in both the MAS and ^1H CPMAS spectra, and their peak intensities were larger in the latter. This supports a model in which the hydroxyls and epoxides are close enough for cross-polarization by the proton in the OH group. This observation is in contrast with previous models.^{8,10,14,17} Both CH_2 and CH_3 groups also appear in both the MAS and ^1H CPMAS spectra but with slightly reduced intensities in ^1H CPMAS, although both have hydrogen atoms nearby. Therefore, CH_2 and CH_3 groups are likely to exist at the edges of the GO flakes. The C=O peak at 212.9 ppm disappears in ^1H CPMAS, and we suggest this argues for its presence primarily at the edges. All six functional groups were also confirmed by FTIR analysis (Supporting Information S2 and S3).

To further assess the functional groups present in each type of sample, XPS data were acquired. The spectra for the GO samples were deconvoluted into four peaks. We observed that in vacuum (SEM and XPS instruments) the GO samples appear to be insulating, because they are clearly charging. Thus, all peak positions were adjusted with respect to the Au 4f peak, because the Au substrate was connected to the GO samples electrically. The C1s peak for sp^2 -hybridized carbon appeared near 285.0 eV in the graphite. After oxidation, the additional peaks were identified as hydroxyl, epoxide, and carboxyl groups attached to the carbon backbone. The sp^2 -hybridized C1s peak intensity was significantly reduced, as shown in Figure 4b. Table 1 summarizes the deconvoluted peak positions and the area relative to the C1s sp^2 peak (expressed as a percentage). When the graphite was oxidized for 24 h (GO1), hydroxyl and epoxide groups were attached to the carbon backbone with an abundance of COOH groups. However, in the second oxidation step (GO2), hydroxyl and carboxyl groups were transformed into epoxide, as illustrated in Table 1 (compare the numbers in parentheses). When the GO1 was heat-treated (GO1_200C), the areas of all the peaks associated with the aforementioned functional groups

(15) Honotiora-Lucas, C.; Lopex-Peinada, A. J.; Lopex-Gonzalez, J. D.; Rojas-Cervantes, M. L.; Martin-Aranda, R. M. *Carbon* **1995**, *33*, 1585–1592.
 (16) Nakajima, T.; Matsuo, A. *Carbon* **1988**, *26*, 357–361.

(17) Nakajima, T.; Matsuo, Y. *Carbon* **1994**, *32*, 469–475.

(18) Gruz, F.; Cowley, J. M. *Acta Crystallogr.* **1963**, *16*, 531–534.

Table 1. XPS Data of C1s of GOs Deconvoluted into Four Peaks; Binding Energies and Relative Area Percentages with Respect to C–C Bonds in Parentheses

sample	C–C	C–OH	O–C–O	HO–C=O
PG	285.0			
GO1	285.1 (100)	286.9 (76)	287.6 (36)	289.0 (217)
GO2	284.9 (100)	286.5 (12)	287.8 (46)	289.6 (31)
GO1_200C	285.1 (100)	286.3 (20)	287.2 (30)	289.0 (21)

Table 2. Atomic Ratios of C/O, H/O, Water Content, and Possible Chemical Formulas from the Elemental Analysis

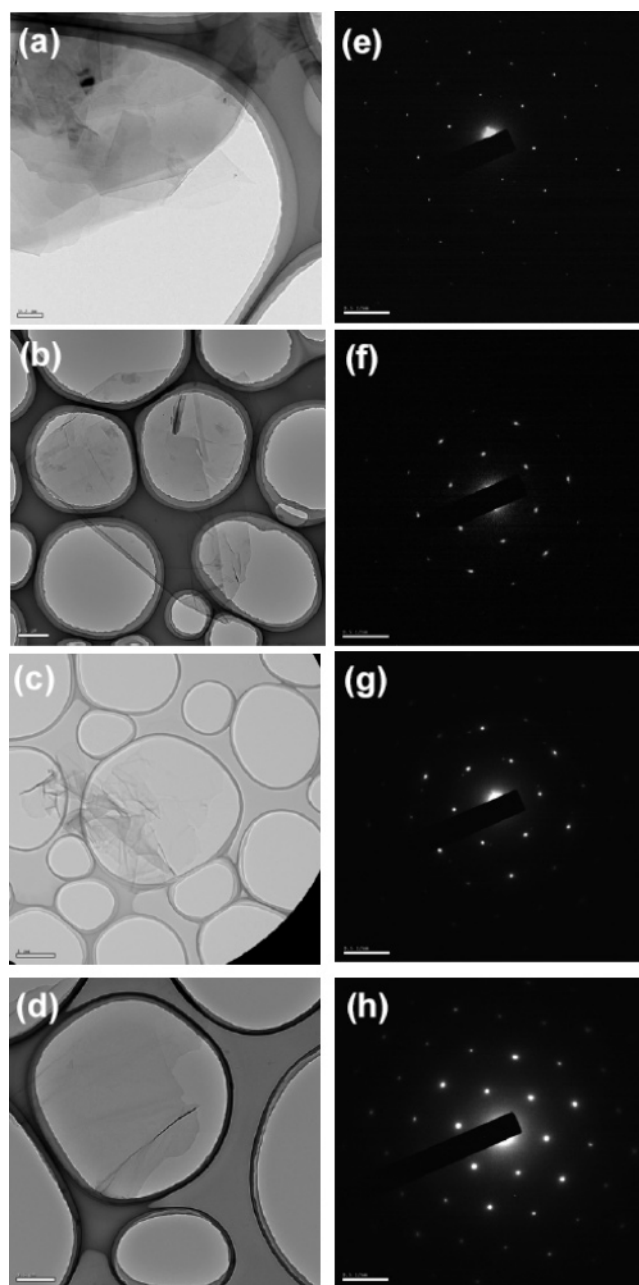
sample	C/O	H/O	water (wt %)	chemical formula
PG	NA	NA	NA	C
GO1	2.64	0.94	7.4	$C_8O_{0.79}(OH)_{1.64}(H_2O)_{0.61}$
GO2	2.47	0.92	9.6	$C_8O_{1.06}(OH)_{1.37}(H_2O)_{0.80}$
GO1_200C	3.19	0.95	6.5	$C_8O_{0.63}(OH)_{1.38}(H_2O)_{0.50}$

including epoxide were reduced relative to the areas of the peaks associated with C–C bonds, and hydroxyl groups were evidently most strongly diminished compared to the epoxide groups. Nevertheless, this trend of removing functional groups upon annealing was similar to those in GO2. The removal of functional groups could also be confirmed from the development of a shoulder near 18° (~ 5 Å) in the XRD measurement of GO2.

The conclusions drawn from XPS and NMR measurements can be summarized as follows. At an early stage of oxidation, graphite is oxidized by forming proximate epoxide and hydroxyl groups in the basal plane such that they are robustly exfoliated. Some of the open edges are also functionalized. When all the available sites are functionalized to form epoxide, the excess oxidant attacks the pre-existing functional groups, particularly hydroxyl and carboxyl groups at the edges. Thus, the oxidation and reduction process is in equilibrium so that the expansion of the interlayer distance cannot continue any further.

Elemental analysis of the GO samples was performed to determine their elemental composition as shown in Table 2. From the experimental atomic ratios of C/O and H/O, we could deduce a possible chemical formula for the different graphite oxides (the water content was obtained from TGA; Supporting Information S4). The chemical formula of GO1 was determined to be $C_8O_{0.79}(OH)_{1.64}(H_2O)_{0.61}$. After the second oxidation step, the composition was $C_8O_{1.06}(OH)_{1.37}(H_2O)_{0.80}$; thus, the epoxide groups increased in GO2, but the hydroxyl groups decreased. This is consistent with the XPS results. In this vein, the chemical formula of GO1_200C is $C_8O_{0.63}(OH)_{1.38}(H_2O)_{0.50}$, representing a reduction of the hydroxyl groups after heat treatment as compared to that of GO1. For GO1_200C, the amount of hydrogen atoms is reduced more severely than that of oxygen atoms. This might be related to the weaker binding energy of the hydroxyl group (~ 0.7 eV) than that of the epoxide functional group (~ 2 eV) to the carbon atoms in graphite oxide.¹⁹

TEM images and SAED patterns are presented in Figure 5. The graphene and GO layers between grid lines were clearly seen in all samples. In fact, oxidation involves severe exfoliation of the graphite, yielding fragmented GO flakes. Heavier oxidation (GO2) reduces the size of the flakes, as shown in Figure 5c. The SAED pattern of graphite (Figure 5e) shows a

**Figure 5.** TEM images (a–d) and the corresponding SAED (e–h). The PG (a, e), GO1 (b, f), GO2 (c, g), and GO1_200C (d, h) are shown, respectively. The scale bars of TEM images are 0.2, 0.5, 1, and $0.5 \mu\text{m}$ for PG, GO1, GO2, and GO1_200C, respectively, and the scale bar of SAED is 0.5 nm^{-1} .

perfect hexagonal structure with the AB stacking as expected (i.e., bright spots in a triangular geometry). One intriguing observation in Figure 5f–h is that the hexagonal structures with AB stacking order were still preserved even after the oxidation steps and heat treatment. The size of the spots in the diffraction pattern indicates the fluctuation of carbon positions and that they are larger than those of the precursor graphite. The size of the unit cell (i.e., the area of six triangles) of the graphite oxides is similar to that of precursor graphite within a fluctuation of about ± 0.12 Å, while the graphite has a fluctuation of ± 0.06 Å. It seems that the fluctuations estimated from SAED in TEM were much larger than those obtained by analysis of the XRD data. We note that the observed GO flake in TEM showed clear oxygen peak near 550 eV in low-energy electron energy loss

(19) Lahaye, R. J. W. E.; Jeong, H. K.; Lee, Y. H. Sungkyunkwan University, Suwon, Korea, 2007. Unpublished work.

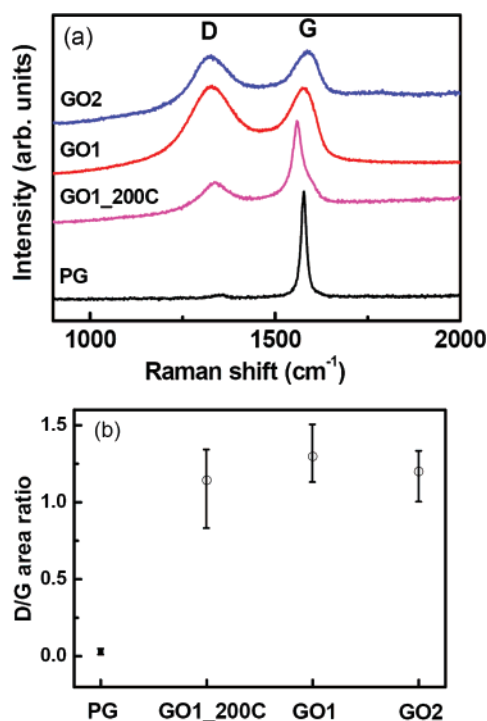


Figure 6. (a) Raman spectra at an excitation wavelength of 514 nm and (b) area ratio of D-band intensity to G-band intensity of each sample.

spectroscopy (not shown here) with an oxygen content of 13 atom %. Therefore, it is certain that the hexagonal AB stacking order originates from GO.

This large fluctuation may originate from the presence of epoxide and hydroxyl groups that involves strains in C–C bonds. The thermal treatment at 200 °C did not seem to change this fluctuation appreciably, as shown in Figure 5. This suggests that even though the functional groups such as epoxide and hydroxyl groups could be incorporated in the graphene network during oxidation, the lattice distortion should be limited within the fluctuation regime. Therefore, relatively small deformation of the carbon network is expected. The functional groups are evidently distributed randomly rather than periodically since there is no indication of spots from the functional groups in the diffraction patterns. Another interesting result from the diffraction spot pattern is identification of the AB stacking order of the GO samples studied here, such as is present in the precursor graphite. The triangular shape was preserved in the diffraction spots, which provides evidence of the AB stacking order. Therefore, we conclude that the GO samples maintain a carbon backbone like in precursor graphite, despite the oxidation or heat treatment at 200 °C under Ar(g), and AB stacking order of the layers is preserved resembling the precursor graphite.

The incorporation of the functional groups could also be identified in Raman spectra, as shown in Figure 6. For the precursor graphite, the G-band around 1600 cm^{-1} that arises from the hexagonal vibration and no appreciable D-band that would identify defects and sp^3 -hybridized bonds clearly indicate high crystallinity and nearly or perhaps completely defect-free graphene layers. With oxidation, the D-band around 1300 cm^{-1} is found. This D-band, however, did not grow relatively larger with longer oxidation (GO1 and GO2), as the D/G peak area ratio remained essentially constant. After heat treatment of GO1, the G-band became sharper than that of GO1, and the intensity of the D band seemed to be decreased slightly compared to that of GO1. The appearance and relative magnitude of the D-band in the Raman spectra for the oxidized samples suggests incorporation of functional groups in the carbon backbone, in agreement with the conclusions reached from analysis of the NMR and XPS data.

IV. Conclusions

GOs have been synthesized by a simplified version of Brodie's method and characterized by the combined methods such as EA, XRD, SEM, TEM, Raman spectroscopy, FTIR, ^{13}C NMR, and XPS. Interlayer distances of GOs were around 7.0 ± 0.35 Å from XRD. The most interesting feature of GOs is that layered textures of GOs were well preserved with a clear AB stacking order and a hexagonal structure in the plane with functional groups such as hydroxyl, epoxide, carboxyl, and some alkyl groups that are distributed randomly. The hydroxyl and epoxide functional groups were located on their basal planes close to each other, while the carboxyl and alkyl groups were likely located at the edges of the GO flakes. With longer oxidation times, hydroxyl groups were transformed into more epoxide groups in the basal plane. Our finding of the graphitic structure of GOs with an AB stacking order will provide positive features in the potential graphene applications.

Acknowledgment. This work was supported by the STAR faculty project in the Ministry of Education, and KOSEF through CNNC at SKKU. We thank CCRF at SKKU, NCIRF at SNU, and KBSI at Dagu for helpful discussions on each measurement. R.S.R. thanks DARPA support for the DARPA Center on Nanoscale Science and Technology for Integrated Micro/NanoElectromechanical Transducers (iMINT) (Award No. HR0011-06-1-0048).

Supporting Information Available: Analytical and spectral characterization data of XRD, FTIR, and TGA experiments. This material is available free of charge via the Internet at <http://pubs.acs.org>.

JA076473O